iScience, Volume *25*

Supplemental information

Engineering rotating apical-out airway organoid for assessing respiratory cilia motility

Piyumi Wijesekara, Prakarsh Yadav, Lydia A. Perkins, Donna B. Stolz, Jonathan M. Franks, Simon C. Watkins, Emily Reinoso Jacome, Steven L. Brody, Amjad Horani, Jian Xu, Amir Barati Farimani, and Xi Ren

List of Supplementary Information:

Supplementary Figure 1. Airway organoid formation in different media in 3D suspension culture. Related to Figure 1.

Supplementary Figure 2. Immunofluorescence images of day-1, 3, 7, 14, and 21 AOAOs stained for FOXJ1. Related to Figure 1.

Supplementary Figure 3. Immunofluorescence images of day-1, 3, 7, 14, and 21 AOAOs stained for Ac-α-Tub. Related to Figure 1.

Supplementary Figure 4. Immunofluorescence images of day-1, 3, 7, 14, and 21 AOAOs stained for ZO-1. Related to Figure 1.

Supplementary Figure 5. Percentage ciliation of day-21 and day-28 AOAOs. Related to Figure 1.

Supplementary Figure 6. Immunofluorescence staining of P63 in mature AOAOs and day-1 organoids. Related to Figure 1.

Supplementary Figure 7. Immunofluorescence staining of CCSP in mature AOAOs and differentiated airway epithelium from air-liquid-interface culture. Related to Figure 1.

Supplementary Figure 8. Characterizing cellular composition in AOAOs differentiated in the presence and absence of IL-13. Related to Figure 1.

Supplementary Figure 9. Immunofluorescence images of day-21 organoids subjected to two-phase culture procedure (1 day in suspension followed by 20 days in Matrigel embedding) and stained for FOXJ1, Ac-α-Tub, and ZO-1. Related to Figure 2.

Supplementary Figure 10. Large organoid bodies in the organoid culture transferred to Matrigel-embedding following 1 day in suspension from dissociated hABSCs. Related to Figure 2.

Supplementary Figure 11. Tangential and angular speed profiles of AOAO rotation. Related to Figure 3.

Supplementary Figure 12. Tracking the rotational motion of mature AOAOs for an extended timescale of 5 minutes. Related to Figure 3.

Supplementary Figure 13. The projected area distribution of AOAOs used for calculating organoid angular speed following EHNA or control treatment for 2 hours in Figure 4C. Related to Figure 4.

Supplementary Figure 14. The projected area distribution of AOAOs used for calculating the change in organoid angular speed in the presence or absence of 20 μM paclitaxel treatment for 24 hours (Figure 4G). Related to Figure 4.

Supplementary Figure 15. Percentage of ciliated cells after EHNA and paclitaxel treatment. Related to Figure 4.

Supplementary Figure 16. Quantification of cell viability after EHNA and paclitaxel treatment. Related to Figure 4.

Supplementary Figure 17. Immunofluorescence images of day-21 PCD and healthy AOAOs stained for Ac-α-Tub. Related to Figure 5.

Supplementary Figure 18. The projected area distribution of healthy and PCD AOAOs used for calculating the angular speed in Figure 5F and rotation analysis in Figure 5G. Related to Figure 5.

Supplementary Video 1. Day-21 AOAO from 3D suspension culture with cilia beating on its exterior surface. Related to Figure 1 and Figure 3.

Supplementary Video 2. Matrigel-supported rotation of mature AOAO. Related to Figure 3. Mature AOAO formed in 3D suspension culture was transferred to 40% GFR-Matrigel embedding, where the exterior-facing cilia propelled against the Matrigel matrix and drove the organoid to rotate.

Supplementary Video 3. Demonstration of computer vision framework for tracking the rotational motion of AOAOs embedded in Matrigel. Related to Figure 3. The video showed the tracking of organoid rotation for 5 seconds comprising the 4 steps as described in Figure 3D. The first panel showed the raw organoid video with extracted ROI and the fit ellipse to suppress background noise. The second panel showed the implementation of the tracking algorithm and visualization of the trajectory of each correspondence as green trace. The third panel was time-synchronized plot of the instantaneous angular speed of the organoid. The correspondences in panel 2 were recomputed every 1 second to minimize the error accumulation by tracking algorithm. The traces for the trajectory of each correspondence were reset after 1 second and correspondences were recomputed from the new orientation of organoid. The tangential speed for each of the 1-second segments of the organoid video was averaged to find the tangential speed of the organoid over the duration of entire video.

Supplementary Video 4. Tracking the rotational motion of mature AOAO for an extended timescale of 5 minutes. Related to Figure 3.

Supplementary Video 5. Visualization of EHNA modulation of AOAO rotation. Related to Figure 4. The first row showed the rotational motion of mature AOAO before EHNA treatment, and the second row showed the same organoid following 2 hours of EHNA treatment. The first column showed treatment with 0 mM of EHNA (control), and the second column showed treatment with 1 mM of EHNA.

Supplementary Video 6. Tracking the rotational motion of mature AOAOs engineered from healthy and PCD (CCDC39 mutation) hABSCs. Related to Figure 5. The first row showed the healthy AOAO, its tracking demonstration, and the corresponding time-synchronized angular speed plot. The second row showed the PCD AOAO, its tracking demonstration, and the corresponding time-synchronized angular speed plot.

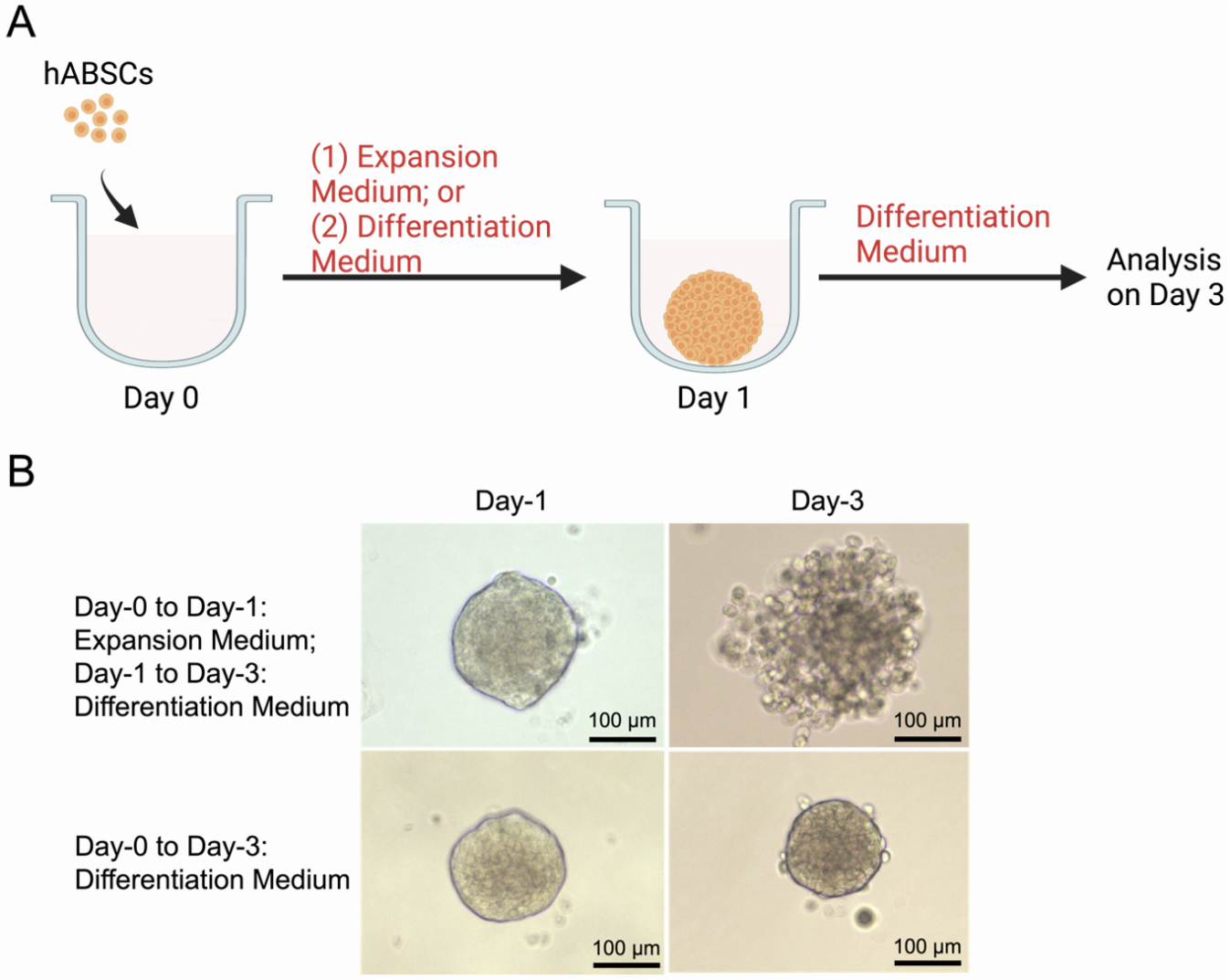

Supplementary Figure 1. Airway organoid formation in different media in 3D suspension culture. Related to Figure 1. (A) Diagram showing the conditions under comparison: during day-0 to day-1 of 3D suspension culture, the organoid was either cultured in BEGM-based expansion medium or in differentiation medium (PneumaCult-ALI); and during day-1 to day-3 of culture, the organoid was cultured in differentiation medium. (B) Brightfield images of organoid integrity on day-1 and day-3 of culture.

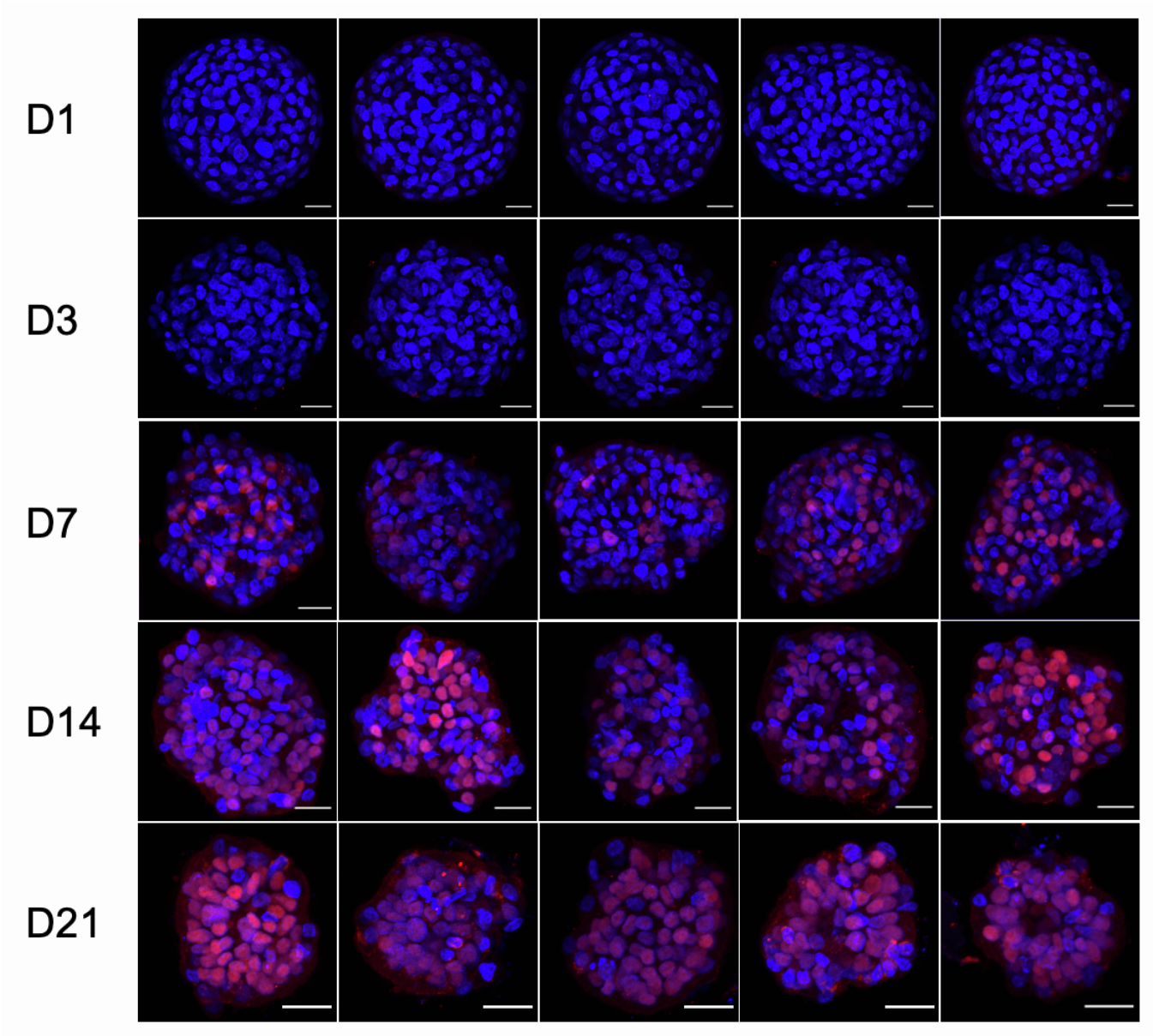

Supplementary Figure 2. Immunofluorescence images of day-1, 3, 7, 14, and 21 AOAOs stained for FOXJ1. Related to Figure 1. Scale bar, 25 μm.

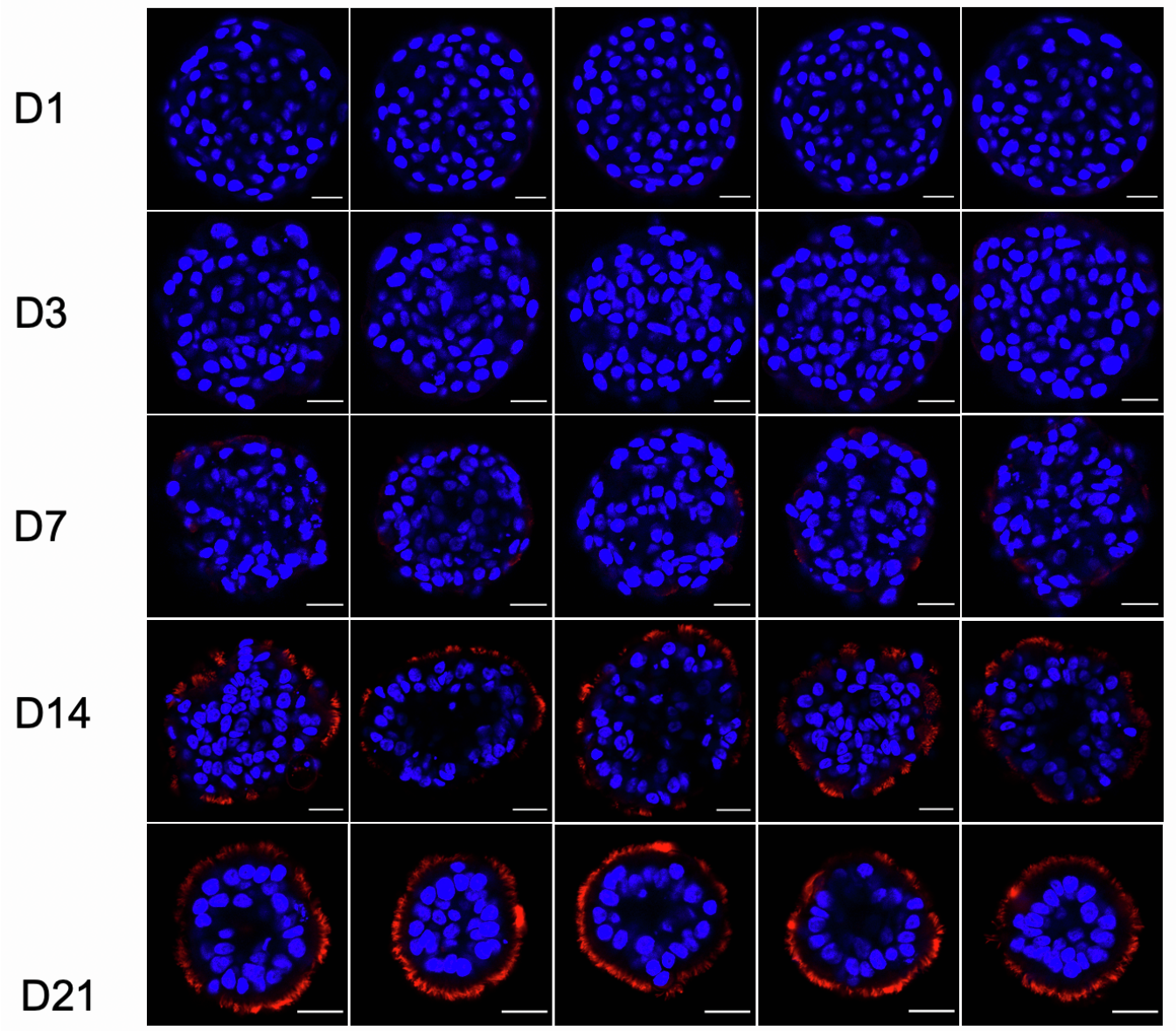

Supplementary Figure 3. Immunofluorescence images of day-1, 3, 7, 14, and 21 AOAOs stained for Ac-α-Tub. Related to Figure 1. Scale bar, 25 μm.

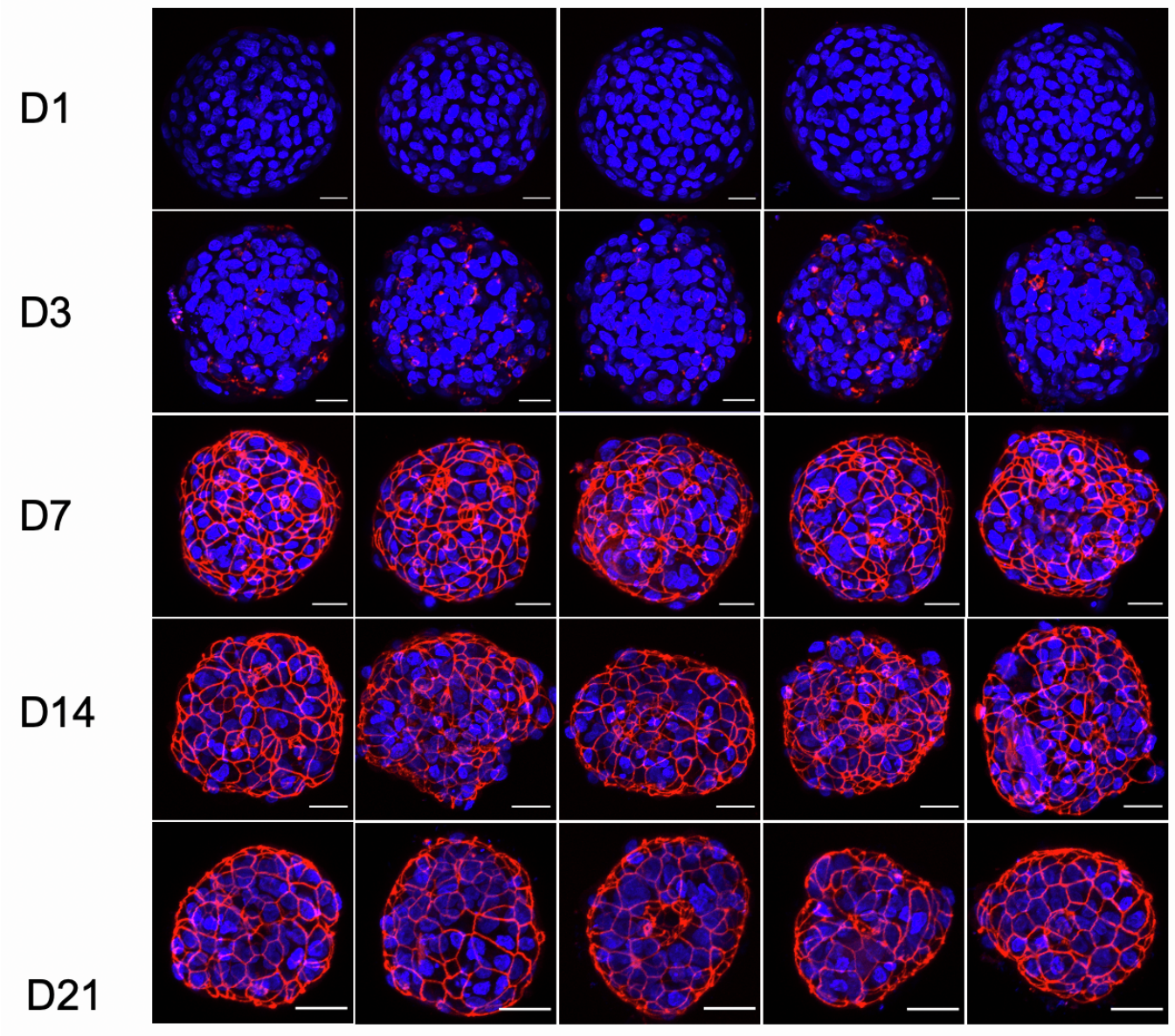

Supplementary Figure 4. Immunofluorescence images of day-1, 3, 7, 14, and 21 AOAOs stained for ZO-1. Related to Figure 1. Scale bar, 25 μm.

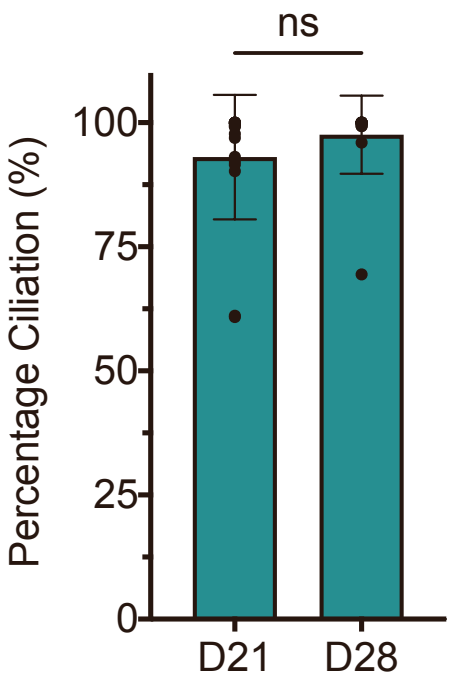

Supplementary Figure 5. Percentage ciliation of day-21 and day-28 AOAOs. Related to Figure 1.
All data represent means ± SD from ≥15 organoids. $*p < 0.05$, $**p < 0.01$, $***p < 0.001$, Unpaired t-test.

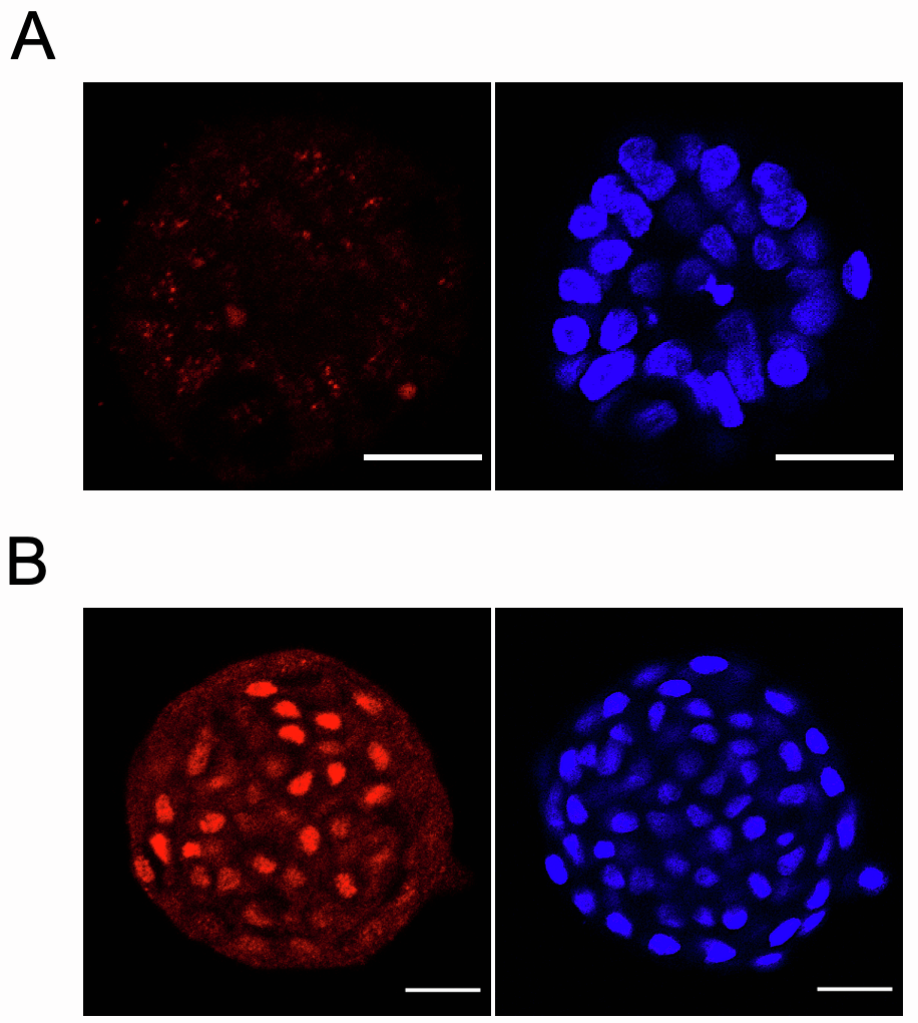

Supplementary Figure 6. Immunofluorescence staining of P63 in mature AOAOs (A) and day-1 organoids (B). Related to Figure 1. Mature AOAOs had no expression of $P63^{+}$ airway basal stem cells compared to day-1 organoids. Scale bar, 25 μm.

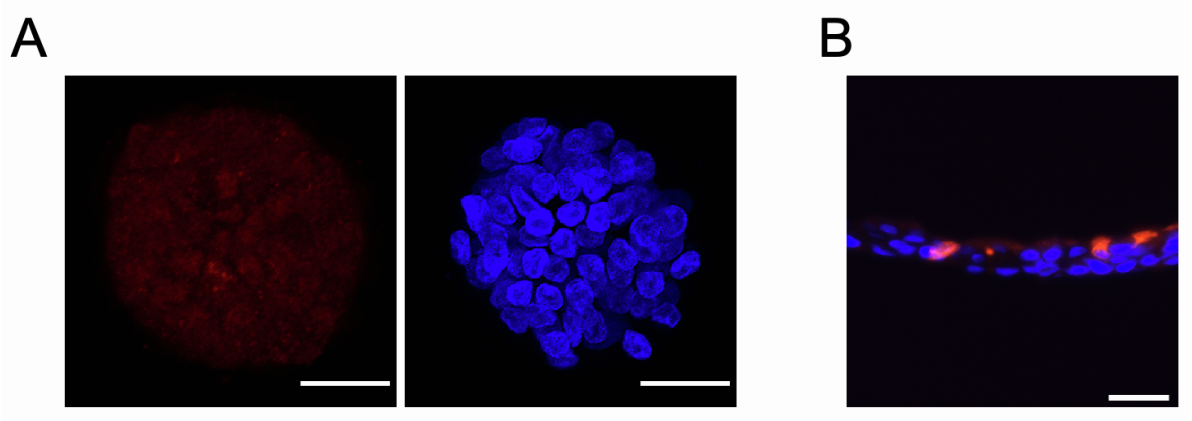

Supplementary Figure 7. Immunofluorescence staining of CCSP in mature AOAOs (A) and differentiated airway epithelium from air-liquid-interface (ALI) culture. Related to Figure 1. Mature AOAOs had no expression of $CCSP^{+}$ club cells compared to the differentiated airway epithelium from ALI culture used as a control. Scale bar, 25 μm.

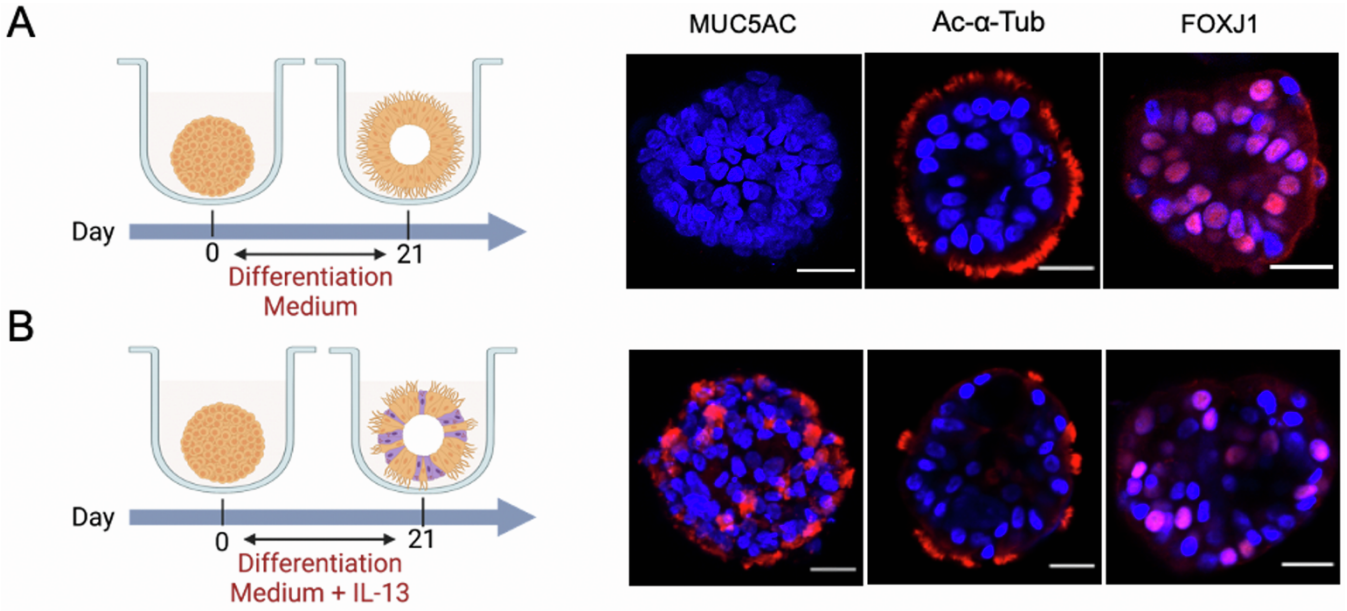

Supplementary Figure 8. Characterizing cellular composition in AOAOs differentiated in the presence and absence of IL-13. Related to Figure 1. (A,B) Immunofluorescence staining of MUC5AC, Ac-α-Tub, and FOXJ1 in AOAOs following 21 days culture in either differentiation medium (A) or in differentiation medium supplemented with IL-13 (5 ng/mL).

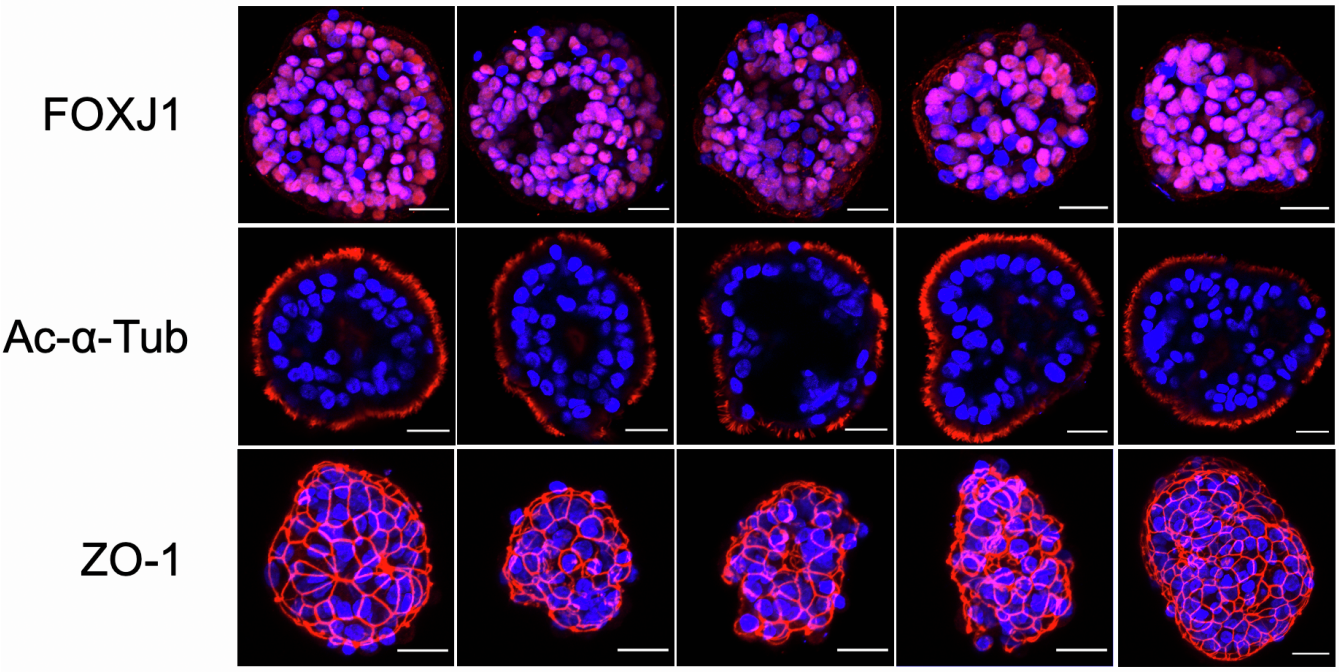

Supplementary Figure 9. Immunofluorescence images of day-21 organoids subjected to two-phase culture procedure (1 day in suspension followed by 20 days in Matrigel embedding) and stained for FOXJ1, Ac-α-Tub, and ZO-1. Related to Figure 2. Scale bar, 25 μm.

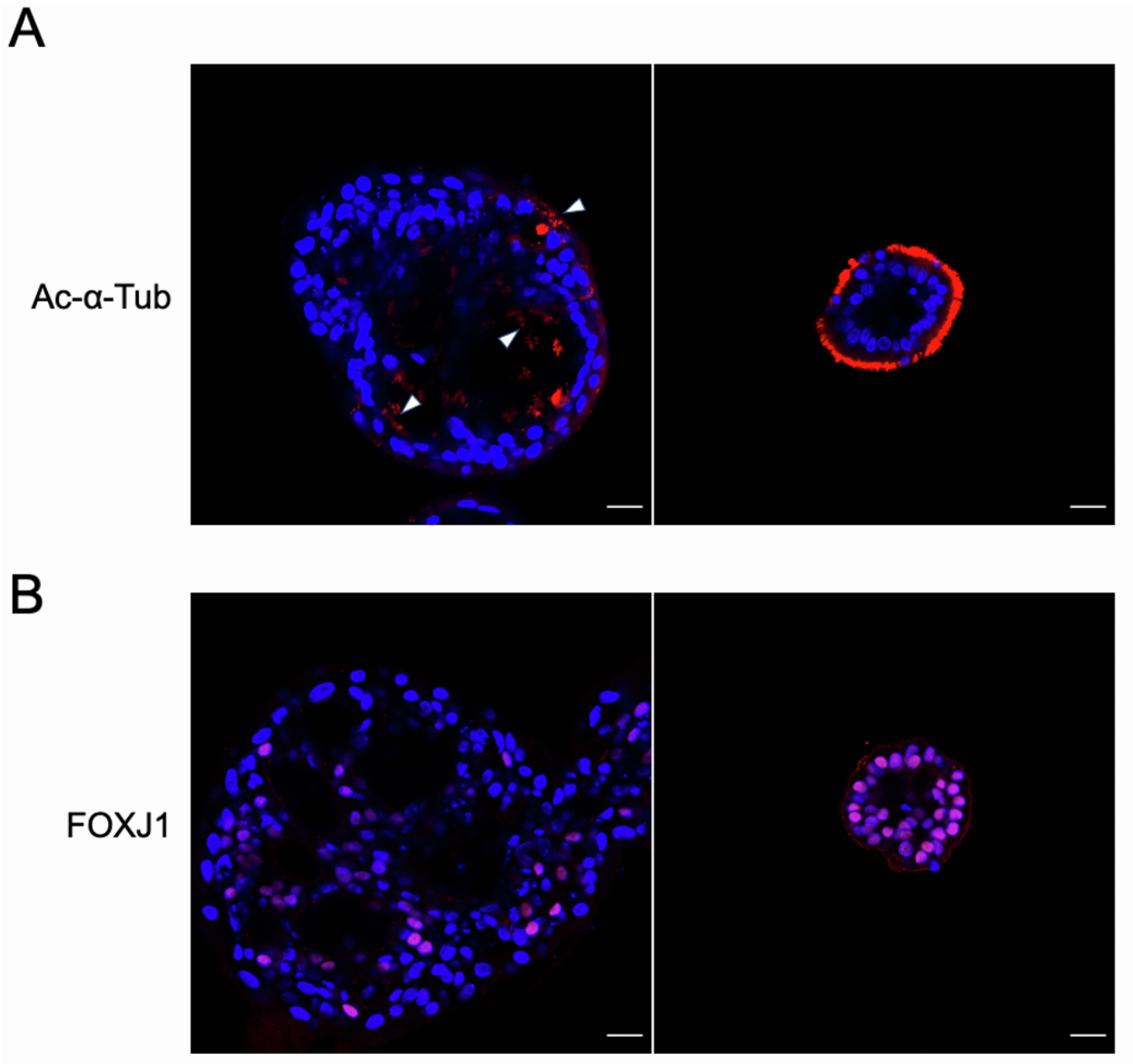

Supplementary Figure 10. Large organoid bodies in the organoid culture transferred to Matrigel-embedding following 1 day in suspension from dissociated hABSCs. Related to Figure 2. (A,B) Immunofluorescence staining of Ac-α-Tub (A) and FOXJ1 (B) in both large organoid bodies and regular-sized organoids on day-21 of culture.

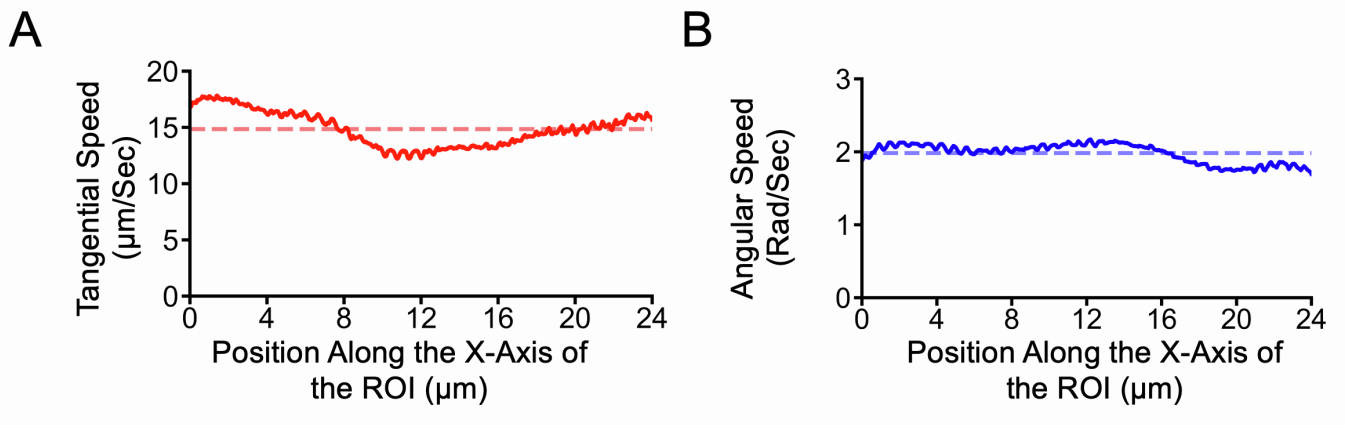

Supplementary Figure 11. Tangential (A) and angular (B) speed profiles of AOAO rotation. **Related to Figure 3.** The solid trace represents the average speed of all correspondences on the organoid perpendicular to that position on the X-axis of the ROI. The dashed line represents the mean speed profile.

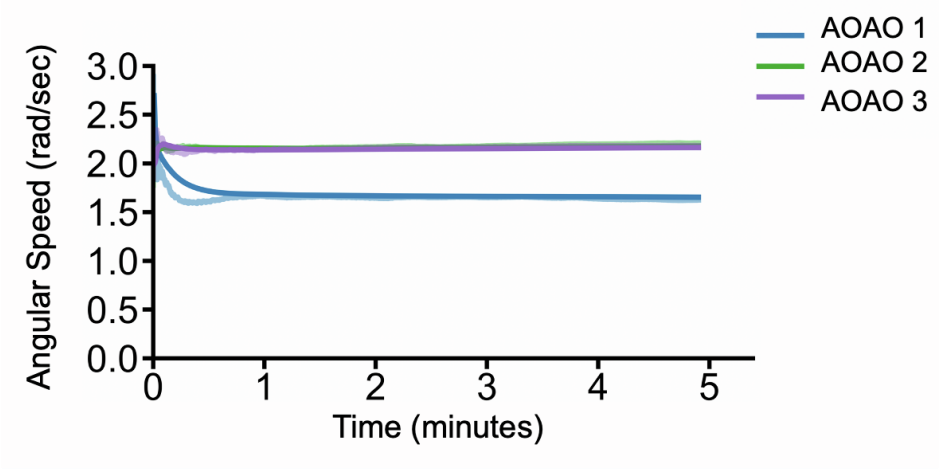

Supplementary Figure 12. Tracking the rotational motion of mature AOAOs for an extended timescale of 5 minutes. Related to Figure 3.

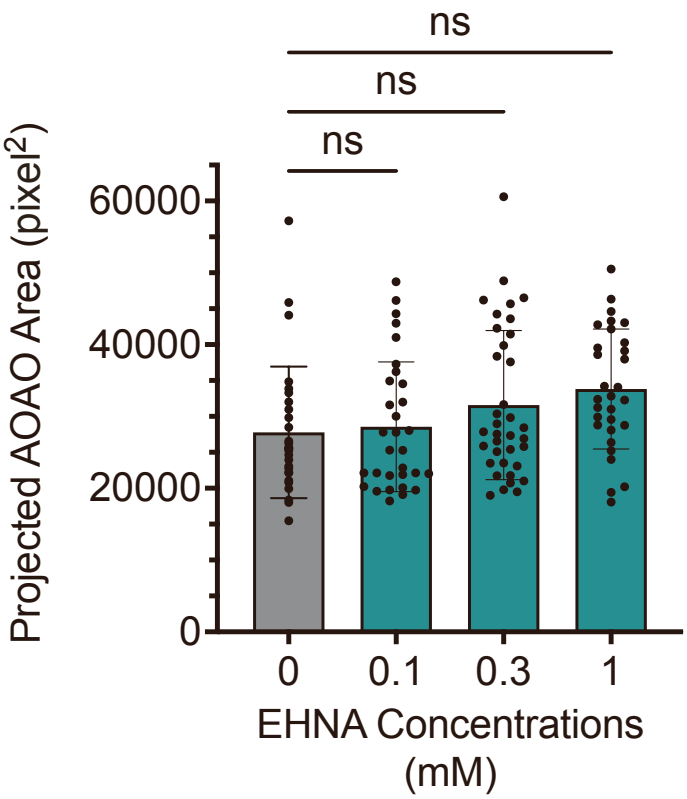

Supplementary Figure 13. The projected area distribution of AOAOs used for calculating organoid angular speed following EHNA or control treatment for 2 hours in Figure 4C. Related to Figure 4.
$*p < 0.05$, $**p < 0.01$, $***p < 0.001$, One-way ANOVA with Tukey's multiple comparisons test.

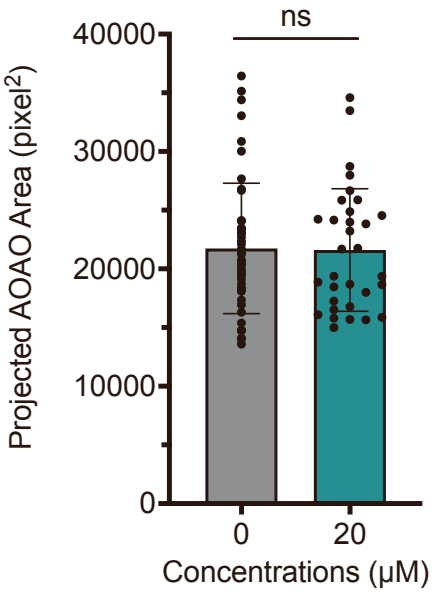

Supplementary Figure 14. The projected area distribution of AOAOs used for calculating the change in organoid angular speed in the presence or absence of 20 μM paclitaxel treatment for 24 hours (Figure 4G). Related to Figure 4. $*p < 0.05$, $**p < 0.01$, $***p < 0.001$, Unpaired t-test.

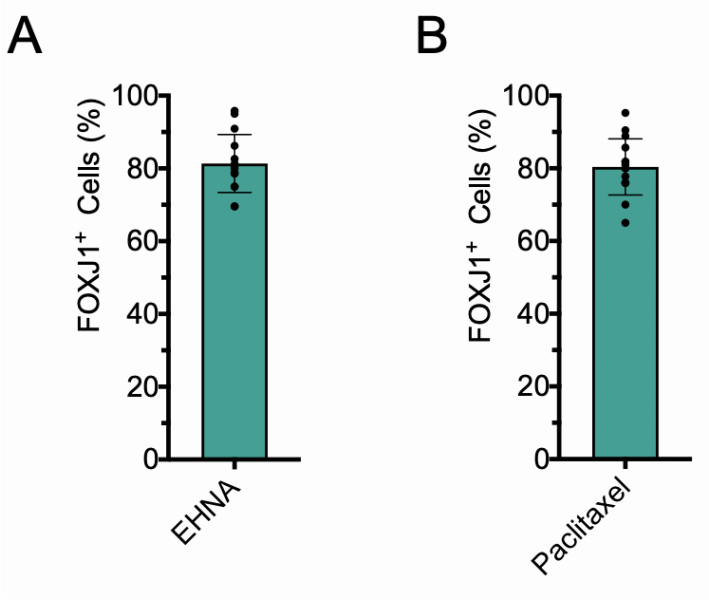

Supplementary Figure 15. Percentage of ciliated cells after EHNA and paclitaxel treatment. Related to Figure 4. After the highest concentrations of (A) EHNA (1 mM) and (B) paclitaxel (20 μM) treatment, the AOAOs were fixed, stained, and quantified for FOXJ1^{+} ciliated cells. The percentage of FOXJ1+ ciliated cells was not significantly different comparing EHNA (1 mM) versus untreated control (p=0.6623), or comparing paclitaxel (20 μM) versus untreated control (p=0.4521).

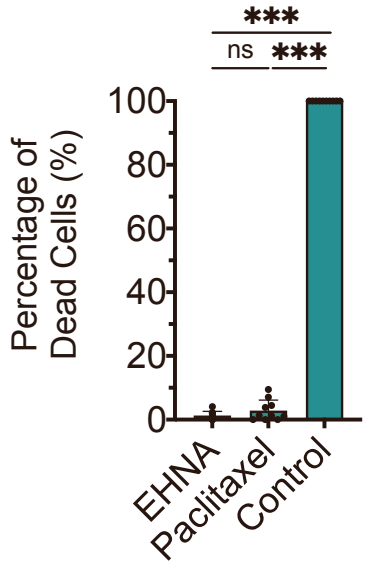

Supplementary Figure 16. Quantification of cell viability after EHNA and paclitaxel treatment. Related to Figure 4. After the highest doses of EHNA (1 mM) and paclitaxel (20 μM) treatment, the AOAOs were stained with a live/dead stain for the quantification of dead cells. Paraformaldehyde (PFA)-fixed AOAOs were used as a control for cell death. All data represent means ± SD from 10 organoids. $*p < 0.05$, $**p < 0.01$, $***p < 0.001$, One-way ANOVA with Tukey's multiple comparisons test.

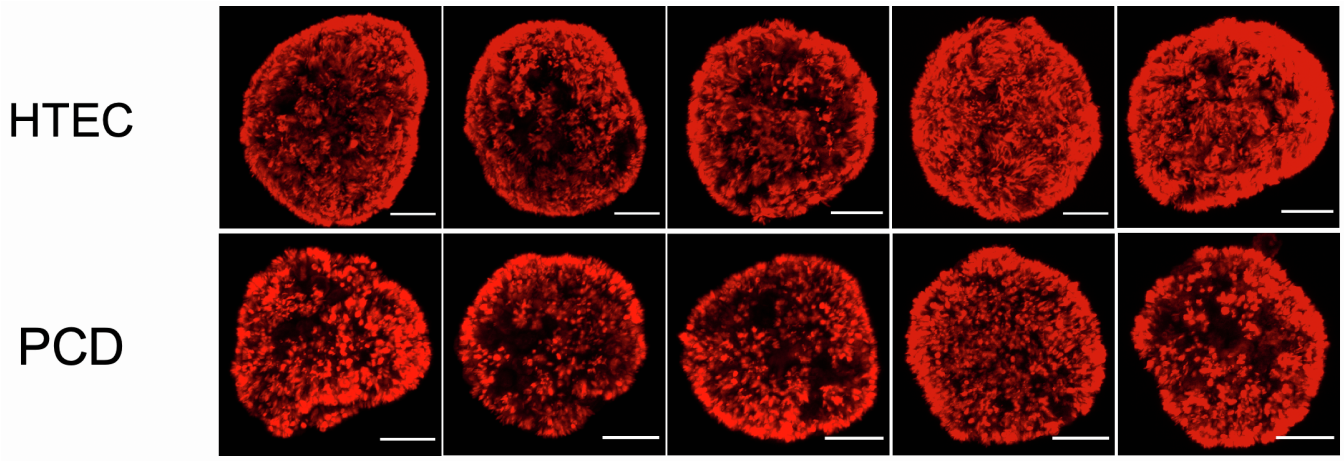

Supplementary Figure 17. Immunofluorescence images of day-21 PCD and healthy AOAOs stained for Ac-α-Tub. Related to Figure 5. Scale bar, 25 μm.

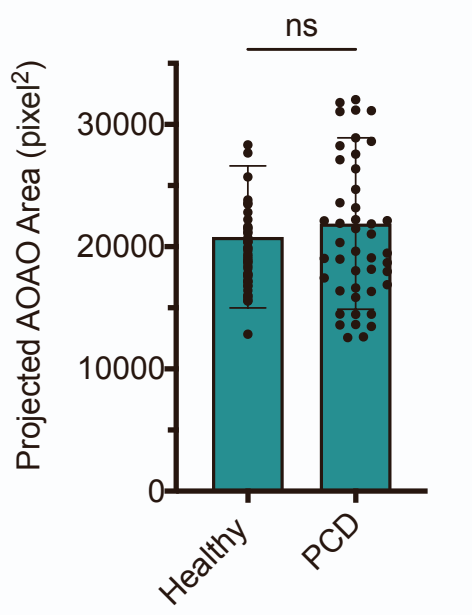

Supplementary Figure 18. The projected area distribution of healthy and PCD AOAOs used for calculating the angular speed in Figure 5F and rotation analysis in Figure 5G. Related to Figure 5. $*p < 0.05$, $**p < 0.01$, $***p < 0.001$, Unpaired t-test.